Electric Vehicle Cornering Stiffness & Lateral States Estimation Using Synchronized Adaptive Sliding Mode Observer and Kalman Filter

Junaid Iqbal[1*], Khalil Muhammad Zuhaib[2], Ahsin Murtaza Bughio[3], Syed Abid Ali Shah[4], and Muhammad Tarique Bhatti[1]

[1] *Department of Mechanical Engineering, QUEST, Larkana-Campus, PAKISTAN.*

[2] *Department of Electronic Engineering, QUEST, Larkana-Campus, PAKISTAN.*

[3] *Department of Electronic Engineering, QUEST, Nawabshah-Campus, PAKISTAN.*

[4] *Department of Electrical Engineering, QUEST, Larkana-Campus, PAKISTAN.*

*Corresponding Author (Email: Jibssp @ gmail.com).

Abstract

The information of tire cornering stiffness and lateral states plays a key role in driver-assist technology. However, this information does not remain the same; and varies with the tire-road condition and driving environment. Therefore, in this paper, a robust estimator scheme is established to adapt the varying tire-road conditions; and estimate the real-time information of tire cornering stiffness and lateral states of an Electric Vehicle (EV). Then, the proposed scheme's estimation accuracy is evaluated over two different driving tests, in which varying tire-road conditions are simulated along with distinct steering inputs. Finally, the simulation results exhibited an excellent estimation performance against uncertain driving conditions.

Disciplinary: Electric Vehicle Engineering and Technology, Mechanical Engineering, Electronics Engineering.
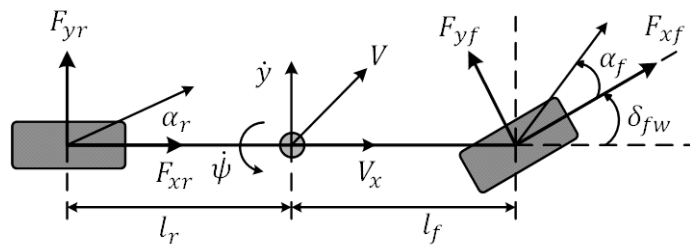
Cite This Article:

1 Introduction

In recent years, Electric Vehicles (EVs) have gained massive attention in the automotive industry due it is environment-friendly nature and lower running cost. In EVs (Anwar & Chen, 2007; Kim et al., 2011; Mihály et al., 2014), the real-time information of the tire cornering stiffness

coefficient and lateral states is a critical factor for incorporating the technologies, i.e. driver assist systems (Gietelink et al., 2006), drive-by-wire systems (Fukao et al., 2004; Pastorino et al., 2011; Ulrich, 2013; Wang et al., 2015) and automated driving (USDOT, 2020; SAE, 2014). However, this information does not remain the same and varies with the tire-road condition and driving environment. Therefore, many researchers have proposed different techniques for estimating the cornering stiffness coefficients and lateral states.

In this regard, nonlinear observers (Amara et al., 2020) and Kalman Filter (KF) (Aydogdu & Levent, 2019; Witchayangkoon, 2000) based estimators have captured significant attention, such as, Hong et al. (2015) estimated 5-DOF vehicle states and parameters over the fixed steering input and constant tire-road conditions by using dual unscented KF. In (Rezaeian et al., 2013; Wenzel et al., 2006), the authors proposed dual extended KF to estimate the road friction and vehicle states. In (Imsland et al., 2006; Oh & Choi, 2012; Zhao et al., 2011), a nonlinear observer is designed with constant gain to observe longitudinal and lateral velocities. However, the observer gains should be selected to cope with the tire-road variations and driving environment.

In this study, we have established an adaptive estimator scheme to adapt the tire-road variations and estimate the cornering coefficients and lateral states of EV by using the synchronized adaptive sliding mode observer (ASMO) (Du et al., 2016) and KF. In this scheme, the termination bounds are incorporated to prevent the estimator from overestimation and saturation. Finally, the estimation accuracy of the proposed scheme is investigated over varying tire-road conditions with distinct steering inputs.

Figure 1: Bicycle Model.

2 EV Lateral Dynamics

In this paper, a continuous-time bicycle model is used to mimic the two-track EV model, see Figure 1. The model consists of 2-degree of freedom represented as lateral velocity $\dot{y}$ and yaw rate $\dot{\psi}$. For the lateral dynamics model, the longitudinal forces F_{xf}, F_{xr} are considered as zero by small-angle approx. i.e., $\cos\theta \approx 1, \sin\theta \approx 0$. Thus, the simplified lateral dynamics is defined as (Abe, 2015; Pacejka & Besselink, 2012; Rajamani, 2012)

$$m(\ddot{y} + V_x\dot{\psi}) = F_{yf} + F_{yr} \tag{1},$$

$$I_z\ddot{\psi} = l_f F_{yf} - l_r F_{yr} \tag{2},$$

where, m, Iz are EV mass and moment of inertia, $\ddot{y}, \ddot{\psi}$ are lateral and yaw acceleration, l_f, l_r is the distance of the center of gravity from the front and rear axle; and δ_{fw}, is EV's front wheel angle, respectively. For small slip angles α_f, α_r, the lateral forces F_{yf}, F_{yr} can be written as

$$F_{yf} = 2C_f \left(\delta_{fw} - \frac{\dot{y} + l_f \dot{\psi}}{V_x} \right) \tag{3},$$

$$F_{yr} = 2C_r \left(-\frac{\dot{y} - l_r \dot{\psi}}{V_x} \right) \tag{4}.$$

Therefore, from Equations (1) to (4), the state-space model is represented as

$$\dot{x} = Mx + N\delta_{fw} \tag{5},$$

where

$$M = \begin{bmatrix} -2\left(\frac{C_f + C_r}{mV_x}\right) & -\left(V_x + 2\left(\frac{l_f C_f - l_r C_r}{mV_x}\right)\right) \\ -2\left(\frac{l_f C_f - l_r C_r}{I_z V_x}\right) & -2\left(\frac{l_f^2 C_f + l_r^2 C_r}{I_z V_x}\right) \end{bmatrix} \tag{6}.$$

$$x = \begin{bmatrix} \dot{y} \\ \dot{\psi} \end{bmatrix}, \quad N = \begin{bmatrix} \frac{2C_f}{m} \\ \frac{2l_f C_f}{I_z} \end{bmatrix} \tag{7}$$

3 Synchronized Estimator Design

Initially, we have designed the ASMO to observe the yaw-rate $\dot{\psi}$, and lateral-velocity $\dot{y}$; and then the KF is synchronized in parallel with the ASMO for estimating the cornering stiffness coefficients over the variable tire-road condition. The synchronized estimation framework is represented in Figure 2.

It is considered that the EV is equipped with sensors, such as the yaw rate $\dot{\psi}$ and lateral acceleration a_y are measured from IMU (Inertial Measurement Unit); and V_x is obtained from a longitudinal speed sensor and wheel encoders. Moreover, the measurement model of lateral acceleration a_y, is defined as (Hong et al., 2015)

$$a_{y,\text{mes}} = \ddot{y} + V_x \dot{\psi} \tag{8}.$$

Furthermore, the lateral velocity is obtained by an integral strap-down model (Woodman, 2007) formulated as

$$\dot{y}(t) = \dot{y}(k-1) + \int (a_{y,\text{mes}} - V_x \dot{\psi}) dk \tag{9},$$

where $\dot{y}(k-1)$ is the lateral velocity at an instant $(k-1)$.

The integral strap-down of $(a_{y,\text{mes}} - V_x \dot{\psi})$ lateral acceleration might integrate the small measurement noise, and the ASMO estimation can diverge over time. Therefore, a small forgetting factor σ (Benoussaad et al., 2015), is added to cancel out the measurement model's small noise. Thus, the integral strap-down model can be written as
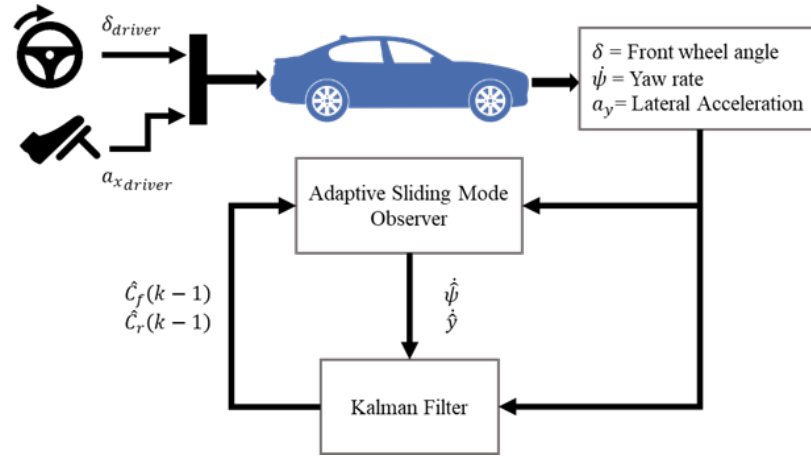
$$\dot{y}(t) = \dot{y}(k-1)(1-\sigma) + \int (a_{y,\text{mes}} - V_x \dot{\psi}) dk \tag{10}.$$

To observe the lateral states of EV Equation (5); the generalized sliding mode observer (SMO) can be formulated as

$$\ddot{\hat{y}} = -\left(M_{11}\dot{\hat{y}} + M_{12}\dot{\hat{\psi}}\right) + N_1\delta_{fw} + K_1\text{sign}(e_1) \tag{11},$$

$$\ddot{\hat{\psi}} = -\left(M_{21}\dot{\hat{y}} + M_{22}\dot{\hat{\psi}}\right) + N_2\delta_{fw} + K_2\text{sign}(e_2) \tag{12},$$

where $e_1 = \dot{y} - \dot{\hat{y}}$, $e_2 = \dot{\psi} - \dot{\hat{\psi}}$; M_{11}, M_{12}, N_1, N_2 are the elements of state-space model Equation (6), such as, m_0 and I_{z0}, are nominal parameters; K_1 and K_2 are the SMO gains, respectively.

Figure 2: Synchronized estimation framework

Therefore, the gains K_1, K_2 must satisfy the given conditions, defined as

$$K_1 > \max\{|M_{11}e_1| + |M_{12}e_2|\} \tag{13},$$

$$K_2 > \max\{|M_{21}e_1| + |M_{22}e_2|\} \tag{14}.$$

The information of tire-road variation and driving environment are the key factors in the SMO design process. However, any inappropriate selection of gains K_1 and K_2, can drastically reduce the performance of SMO, and in consequence, the lateral state estimation can deviate from the trajectory.

In view of the abovementioned facts, the gain-adaptation-based SMO (Du et al., 2016) is proposed in this study. The proposed ASMO has the capability to tackle the uncertain tire-road conditions by adapting the new gains as per driving environment that robustly improves estimation performance. Thus, ASMO based lateral states Equations (11) and (12) are revised as

$$\ddot{\hat{y}} = -\left(M_{11}\dot{\hat{y}} + M_{12}\dot{\hat{\psi}}\right) + N_1\delta_{fw} + \widehat{K}_1(k)\text{sign}(e_1) \tag{15},$$

$$\ddot{\hat{\psi}} = -(M_{21}\dot{\hat{y}} + M_{22}\dot{\hat{\psi}}) + N_2\delta_{fw} + \widehat{K}_2(k)\text{sign}(e_2) \tag{16}.$$

Hence, the gain adaptation law for ASMO is expressed as

$$\dot{\widehat{K}}_i(k) = \begin{cases} \rho_i|e_i|, & |e_i| > \varepsilon_i \\ 0, & \text{otherwise} \end{cases} \tag{17},$$

where $i = 1,2$; $\hat{K}_i(k) > 0$, is a strictly positive adaptive gain; ρ_i, is a strictly positive constant used for adjusting the gain adaption speed; $\varepsilon_i \ll 1$, is an adjustable small positive constant, which is used for activating the gain adaptation mechanism. Therefore, the gain adaptation will be stopped for a finite time when the error extents to selected bound $|e_i| \le \varepsilon_i$ in a finite time.

Hence, to validate the convergence of ASMO; the Lyapunov candidate function V_1 for lateral velocity is selected as

$$V_1 = \frac{1}{2}e_1^2 + \frac{1}{2\rho_1}\tilde{K}_1 \tag{18},$$

where $\tilde{K}_1 = \hat{K}_1 - K_1$, is an adaptive gain convergence error.

Therefore, the time derivative of V_1, is obtained as follows, such that, $\dot{K}_1 = 0$:

$$\dot{V}_1 = e_1\dot{e}_1 + \frac{1}{\rho_1}\tilde{K}_1\dot{\hat{K}}_1$$

$$= -e_1\left[M_{11}e_1 + M_{12}e_2 + \hat{K}_1\,\text{sign}(e_1)\right] + \frac{1}{\rho_1}\tilde{K}_1\dot{\hat{K}}_1 \tag{19}.$$

$$\le -e_1\left[M_{11}e_1 + M_{12}e_2\right] - \hat{K}_1|e_1| + \left(\hat{K}_1 - K_1\right)|e_1|$$
$$\le -e_1\left[M_{11}e_1 + M_{12}e_2\right] - K_1|e_1|$$

Thus, by considering Equation (13),

$$\dot{V}_1 \le 0.$$

Similarly, for yaw rate convergence, the Lyapunov candidate function V_2, is selected as follow, such that, $\dot{K}_2 = 0$:

$$V_2 = \frac{1}{2}e_2^2 + \frac{1}{2\rho_2}\tilde{K}_2 \tag{20}$$

where $\tilde{K}_2 = \hat{K}_2 - K_2$, is an adaptive gain convergence error for V_2. Likewise, the time derivative of V_2, will also asymptotically converge to zero, $\dot{V}_2 \le 0$, by considering Equation (14).

To prevent the ASMO from high-frequency chattering problem; the chattering component sign (e_i) is substituted with the continuous linear function $e_i/(|e_i| + \varepsilon_i)$, such that Equations (15) and (16) can be revised as

$$\ddot{\hat{y}} = -\left(M_{11}\dot{\hat{y}} + M_{12}\dot{\hat{\psi}}\right) + N_1\delta_{fw} + \hat{K}_1(k)\frac{e_1}{|e_1|+\varepsilon_1} \tag{21}$$

$$\ddot{\hat{\psi}} = -(M_{21}\dot{\hat{y}} + M_{22}\dot{\hat{\psi}}) + N_2\delta_{fw} + \hat{K}_2(k)\frac{e_2}{|e_2|+\varepsilon_2} \tag{22}$$

However, the estimation performance of the ASMO is mainly relying on the real-time information of C_f and C_r, front and rear cornering stiffness coefficients; and this information cannot be measured directly from EV's onboard sensors.

Due to this fact, the Kalman filter (KF) (Simon, 2006) is added in parallel to ASMO for estimating the cornering stiffness coefficients under varying tire–road conditions as shown in

Figure 2. Then the sufficient set of estimated coefficients will be feedback to ASMO. The Kalman Filter algorithm (Shin, 2013; Simon, 2006) for cornering stiffness estimation is given as:

1. Initialize:

$\widehat{w}_0 = E[w(0)]$

$P_0 = E[(w(0) - \widehat{w}_0)(w(0) - \widehat{w}_0)^T]$

2. Prediction Update:

$\widehat{w}_k^- = \widehat{w}_{k-1}$

$P_k^- = P_{k-1} + Q$

3. Measurement Update:

$K_k = P_k^- H^T (H P_k^- H^T + R)^{-1}$

$\widehat{w}_k = \widehat{w}_k^- + K_t(z_k - H\widehat{w}_k^-)$

$P_k = (I - K_k H)P_k^-$

where, P, Q, and R, represents the estimation error covariance, process noise covariance, and measurement noise covariance, respectively; and $R = r_s^2$, where r_s, denotes the sensor zero-mean white noise.

The w and z, are defined as tire cornering stiffness coefficient vector and lateral acceleration measurement vector, such that:

$$= \begin{bmatrix} C_f & C_r \end{bmatrix}^T, z = Hw \tag{23}$$

where $z = a_y$

$$H = \left[-\frac{2}{m_0}\left(\frac{\dot{y}+l_f\dot{\psi}}{V_x} - \delta_{fw}\right) \quad -\frac{2}{m_0}\left(\frac{\dot{y}-l_f\dot{\psi}}{V_x}\right) \right] \tag{24}$$

It is to be noted that the w is a constant vector. Therefore, its time derivative is taken as zero ($\dot{w} = 0$). Thus, the Euler's discretized form of w and z, vectors can be defined as

$$w(k) = w(k-1) + q(k) \tag{25}$$

$$z(k) = Hw(k) + r(k) \tag{26}$$

where, q and r, represents the Gaussian white noise and measurement noise, respectively.

For enhancing the convergence accuracy of KF, the residual $e_3 = z_k - H\widehat{w}_k^-$, is utilized to switch on and off the estimator. Therefore, based on e_3, abounded condition is designed, such that, when e_3 extents to specified bound $|e_3| \le \varepsilon_3$, then the KF will switch off, and the estimated parameters will remain constant until and unless e_3, does not exceed the specified bound again. Where ε_3 ($\varepsilon_3 > 0$), is an adjustable positive constant.

Thus, the KF estimation based ASMO for Equations (21) and (22) can be written as

$$\ddot{y} = -M_{11}(\widehat{w}_{k-1})\dot{y} - M_{12}(\widehat{w}_{k-1})\dot{\psi} + N_1(\widehat{w}_{k-1})\delta_{fw} + \widehat{K}_1(k)\frac{e_1}{|e_1|+\varepsilon_1} \tag{27}$$

$$\ddot{\psi} = -M_{21}(\widehat{w}_{k-1})\dot{y} - M_{22}(\widehat{w}_{k-1})\dot{\psi} + N_2(\widehat{w}_{k-1})\delta_{fw} + \widehat{K}_2(k)\frac{e_2}{|e_2|+\varepsilon_2} \tag{28}$$

4 Simulation & Results

In this section, the two distinct driving environments are simulated to evaluate the robustness and estimation accuracy of the synchronized ASMO and KF estimation scheme.
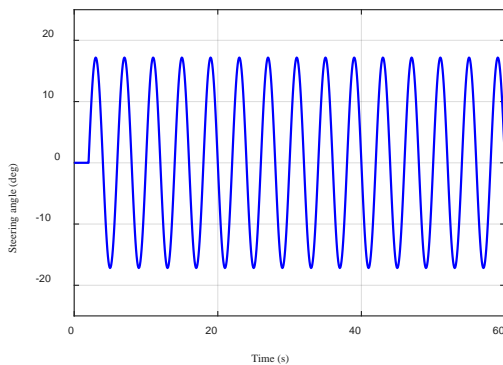
Test#1 is carried out over variable road conditions, such as snowy, wet, and dry road conditions over the selected time range with sine-wave steering input. Test#2 is conducted over constant road conditions with circular steering input and variable longitudinal speed. The EV parameters for the simulation are listed as $m = 1270$ (kg), $I_z = 1537$(kg.m^2), $l_f = 1.015$(m), $l_r = 1.9$(m), and sampling rate Δk is selected as $0.001 s$.

Moreover, the ASMO and KF parameters are chosen as: $\widehat{K}_1(0) = \widehat{K}_2(0) = 7.5$, $\rho_1 = \rho_2 = 9.5$, $\sigma = 0.0015$, $\varepsilon_1 = \varepsilon_2 = 0.006$, residual bound for e_3: $\varepsilon_{\text{lower}} = 8$, $\varepsilon_{upper} = 2600$, $m_0 = 1155$ kg, $I_{z_0} = 1550$ kg.m^2, $\widehat{w}_0 = [175\ 175]^T$, $P_0 = 110000 \times I_{2x2}$, $Q = (10 \times 10^{-6})I_{2\times2}$, and $r_s = 0.0005$.
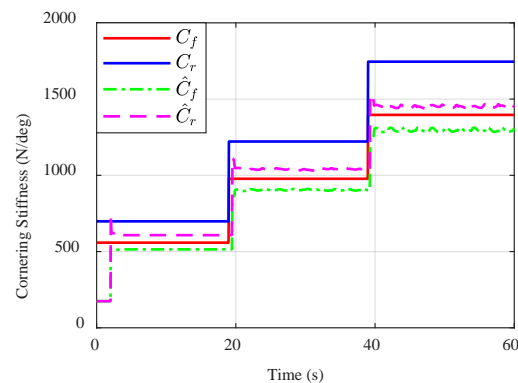
4.1 Variable Road Conditions with Constant Speed Test (Test#1)

For Test#1, variable road conditions are simulated at a constant speed $V_x = 36$ (km/h) for 60 sec and road parameters are selected as snowy road $C_f = 558.5$, $C_r = 698$ (N/deg) for first 20 sec then wet road $C_f = 977.4$, $C_r = 1222$ (N/deg) for next 20 sec and dry road $C_f = 1400$, $C_r = 1745$ (N/deg) for last 20 sec. The sin-wave steering input angle is generated by:
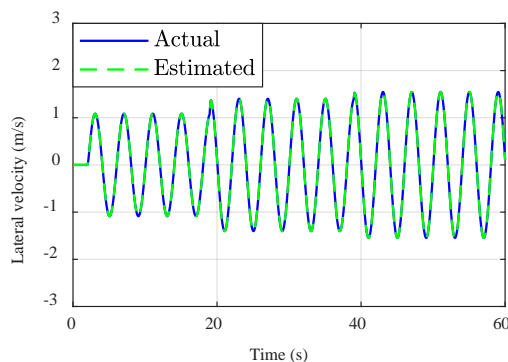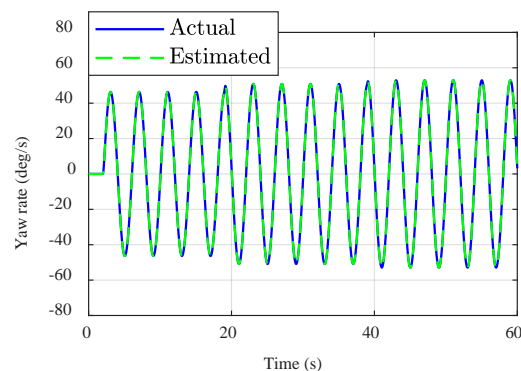
$$\delta_d = 16.5 \sin(0.5\pi k) \text{ deg}$$

Figure 3: Sine-wave steering angle input (Test#1).

Figure 4: Estimated cornering stiffness (Test#1).

Figure 5: Estimated lateral velocity (Test#1).

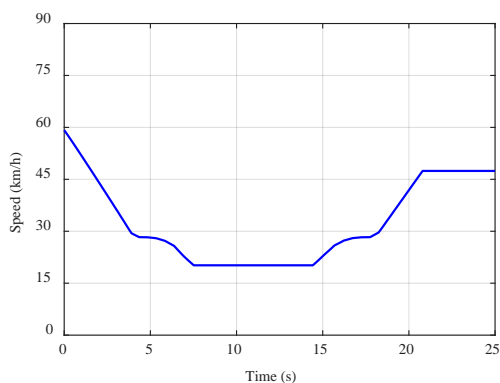**Figure 6**: Estimated yaw rate (Test#1).

We can see from Figures 3-6 that the proposed synchronized ASMO and KF estimator robustly deal with all three road variations; and estimated the cornering coefficients and lateral
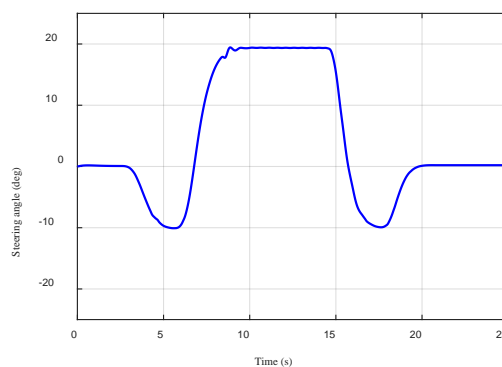
states within the locality of simulated values. Moreover, Figure 4 shows that the estimated cornering coefficients also satisfied the termination bound e_3 and remain persistent in all snowy, wet, and dry road conditions, respectively.

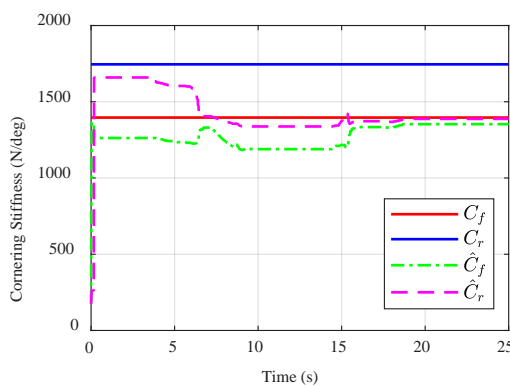## 4.2 Constant Road Condition with Variable Speed Test

This test is conducted over constant road condition such as the dry road parameters are selected as: $C_f = 1400$ (N/deg), $C_r = 1746$ (N/deg). In this test, it also considered that the EV is maneuvering over the circular track by using circular steering input with variable longitudinal speed, as shown in Figures 7 and 8, respectively.
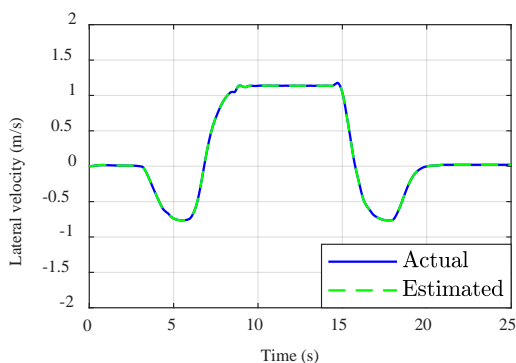

Figure 7: Variable longitudinal speed input (Test#2).
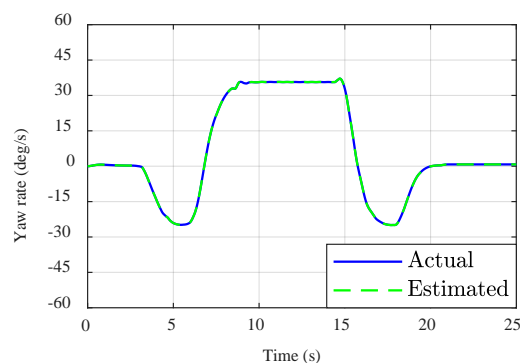

Figure 8: Circular steering angle input (Test#2).

Figure 9: Estimated cornering coefficients (Test#2).

Figure 10: Estimated lateral velocity (Test#2).

Figure 11: Estimated yaw rate (Test#2).

It can be seen from Figure 9 that both the front and rear estimated cornering stiffnesses are not only converged to selected C_f, front stiffness coefficient at variable speed but also prevented the estimator from overestimation. Moreover, in this test the lateral velocity and yaw rate are also estimated very closely, such that, the estimation error remains under bounded condition over the entire circular track as shown in Figures 10–11.

5 Conclusion

In this paper, we have established a synchronized ASMO and KF estimator scheme to estimate the cornering stiffness coefficients and lateral states of EV over variable road conditions with distinct steering inputs. The proposed scheme exhibited robust performance against the driving environment variations in both tests and intelligently estimated the sufficient gains to deal with the snowy, wet and dry road conditions. In simulation and results, it is validated that the estimated lateral states and stiffness coefficients converged to the neighborhood of the simulated system. Moreover, the proposed scheme also satisfied the termination bond conditions that not only prevented the estimator from overestimating the cornering coefficients but also from saturation. Future work should investigate the effect of lateral load shift over split-mu to estimate the nonlinear behavior of lateral states.

6 Availability of Data And Material

Data can be made available by contacting the corresponding author.

7 References

Abe, M. (2015). *Vehicle Handling dynamics : theory and application.* Butterworth-Heinemann.

Amara, H. E., Latreche, S., Sid, M. A., & Khemliche, M. (2020). Sliding Mode Observer and Event Triggering Mechanism Co-design. *Engineering Technology & Applied Science Research*, 10(2), 5487-5491. https://doi.org/10.48084/etasr.3285

Anwar, S., & Chen, L. (2007). An Analytical Redundancy-Based Fault Detection and Isolation Algorithm for a Road-Wheel Control Subsystem in a Steer-By-Wire System. *IEEE Transactions on Vehicular Technology, 56*(5), 2859-2869. https://doi.org/10.1109/TVT.2007.900515

Aydogdu, O., & Levent, M. L. (2019). Kalman State Estimation and LQR Assisted Adaptive Control Of a Variable Loaded Servo System. *Engineering Technology & Applied Science Research, 9*(3), 4125-4130.

Benoussaad, M., Sijobert, B., & Mombaur, K. (2015). Robust foot clearance estimation based on the integration of foot-mounted IMU acceleration data. Sensors. http://www.mdpi.com/1424-8220/16/1/12/htm

Du, J., Liu, Z., Wang, Y., & Wen, C. (2016). An adaptive sliding mode observer for lithium-ion battery state of charge and state of health estimation in electric vehicles. *Control Engineering Practice*. http://www.sciencedirect.com/science/article/pii/S0967066116301149

USDOT. (2020). *Federal Automated Vehicles Policy.* http://www.transportation.gov/AV Accessed 2020.

Fukao, T., Miyasaka, S., Mori, K., Adachi, N., & Osuka, K. (2004). Active Steering Systems Based on Model Reference Adaptive Nonlinear Control. *Vehicle System Dynamics, 42*(5), 301-318. https://doi.org/10.1080/0042311042000266739

Gietelink, O., Ploeg, J., De Schutter, B., & Verhaegen, M. (2006). Development of advanced driver assistance systems with vehicle hardware-in-the-loop simulations. *Vehicle System Dynamics, 44*(7), 569-590. https://doi.org/10.1080/00423110600563338

Hong, S., Lee, C., Borrelli, F., & Hedrick, J. K. (2014). A novel approach for vehicle inertial parameter identification using a dual Kalman filter. *IEEE Transactions on Intelligent Transportation Systems*, 16(1), 151-161.

Imsland, L., Johansen, T. a., Fossen, T. I., Fjær Grip, H., Kalkkuhl, J. C., & Suissa, A. (2006). Vehicle velocity estimation using nonlinear observers. *Automatica, 42*(12), 2091-2103. https://doi.org/10.1016/j.automatica.2006.06.025

Kim, J., Kim, T., Min, B., Hwang, S., & Kim, H. (2011). Mode Control Strategy for a Two-Mode Hybrid Electric Vehicle Using Electrically Variable Transmission (EVT) and Fixed-Gear Mode. *IEEE Transactions on Vehicular Technology, 60*(3), 793-803. https://doi.org/10.1109/TVT.2011.2107564

Mihály, A., Németh, B., & Gáspár, P. (2014). Integrated vehicle control of in-wheel electric vehicle. *Transportation Engineering, 42*(1), 19-25. https://doi.org/10.3311/PPtr.7280

Oh, J. J., & Choi, S. B. (2012). Vehicle velocity observer design using 6-D IMU and multiple-observer approach. *IEEE Transactions on Intelligent Transportation Systems, 13*(4), 1865-1879. https://doi.org/10.1109/TITS.2012.2204984

Pacejka, H. B., & Besselink, I. (2012). *Tire and vehicle dynamics.* Butterworth-Heinemann.

Pastorino, R., Naya, M. A., Pérez, J. A., & Cuadrado, J. (2011). Geared PM coreless motor modelling for driver's force feedback in steer-by-wire systems. *Mechatronics, 21*(6), 1043-1054. https://doi.org/10.1016/j.mechatronics.2011.05.006

Rajamani, R. (2012). *Vehicle Dynamics and Control.* Mechanical Engineering Series in Control.

Rezaeian, A., Zarringhalam, R., Fallah, S., Melek, W., Khajepour, A., Chen, S.-K., & Litkouhi, B. (2013). *Cascaded Dual Extended Kalman Filter for Combined Vehicle State Estimation and Parameter Identification*. https://doi.org/10.4271/2013-01-0691

SAE. (2014). International Technical Standard Provides Terminology for Motor Vehicle Automated Driving Systems. http://www.sae.org/autodrive Accessed 2020.

Shin, D. (2013). Experimental Study on Vehicle to Road Tracking Algorithm by Using Kalman Filter Associated with Vehicle Lateral Dynamics. https://doi.org/10.4271/2013-01-0739

Simon, D. (2006). *Optimal State Estimation: Kalman, H Infinity, and Nonlinear Approaches*. John Wiley. https://doi.org/10.1002/0470045345

Ulrich, L. (2013). Top Tech Cars 2013: Infiniti Q50. *IEEE Spectrum*. http://spectrum.ieee.org/transportation/advanced-cars/infiniti-q50 Accessed 2020.

Wang, H., Xu, Z., Do, M. T., Zheng, J., Cao, Z., & Xie, L. (2015). Neural-network-based robust control for steer-by-wire systems with uncertain dynamics. *Neural Computing and Applications*. https://doi.org/10.1007/s00521-014-1819-2

Wenzel, T. A., Burnham, K. J., Blundell, M. V., & Williams, R. A. (2006). Dual extended Kalman filter for

vehicle state and parameter estimation. *Vehicle System Dynamics, 44*(2), 153-171. https://doi.org/10.1080/00423110500385949

Witchayangkoon, B. (2000). *Elements of GPS precise point positioning*. Ph.D. Thesis, University of Maine, USA.

Woodman, O. (2007). *An introduction to inertial navigation*. http://www.cl.cam.ac.uk/techreports/UCAM-CL-TR-696.html Accessed 2020.

Zhao, L.-H., Liu, Z.-Y., & Chen, H. (2011). Design of a nonlinear observer for vehicle velocity estimation and experiments. *IEEE Transactions on Control Systems Technology, 19*(3), 664-672. https://doi.org/10.1109/TCST.2010.2043104

Dr. Junaid Iqbal is an Assistant Professor at Department of Mechanical Engineering, Quaid-e-Awam University of Engineering, Science & Technology, Larkana – Campus, Pakistan. He got his Bachelor's Degree in Mechanical Engineering and a PhD degree in Mechatronics Engineering form Hanyang University, South Korea. His research focuses on Advanced Vehicle Dynamics & Control, and Robot Control.

Dr. Khalil Muhammad Zuhaib is an Assistant Professor at the Department of Electronic Engineering at Quaid-e-Awam University, Larkana Campus. He got a Bachelor's degree in Electronics Engineering and a Masters's degree Leading to a Ph.D. degree in Mechatronics Engineering from Hanyang University, South Korea. His research interest includes Robot Motion Planning and Multi-Agent Systems.

Dr.Ahsin Murtaza Bughio, received his Ph.D. degree from Politecnico di Torino, Italy. Currently he is an Assistant Professor at Department of Electronic Engineering, Quaid-e-Awam University of Engineering Science & Technology (QUEST), Pakistan. His research interests include RF, FinFETS, Passive Modelling.

Dr. Syed Abid Ali Shah is an Assistant Professor at Department of Electrical Engineering, Quaid-e-Awam University of Engineering, Science & Technology, Larkana – Campus, Pakistan. He got his Bachelor's Degree in Electrical Engineering, Master's Degree in Electrical Power Engineering and a PhD degree in Electrical Machines Design and Optimization from Aston University, Birmingham, United Kingdom. His research interest includes Design and Optimization of Electrical Machines and Drives, and Analysing Especial Machines.

Dr. Muhammad Tarique Bhatti is an Assistant Professor at Department of Mechanical Engineering, Quaid-e-Awam University of Engineering, Science & Technology, Larkana – Campus, Pakistan. He got his Bachelor's Degree in Mechanical Engineering and PhD degree in Advanced Manufacturing Processes from Dublin City University, Ireland. His research focuses on Advanced Methods of Machining, 6 DOF Manufacturing Process and Health & Safety.